

Spectrophotometric behavior of CU Virginis^{*}

N.A. Sokolov^{1,2}

¹ Central Astronomical Observatory at Pulkovo, St. Petersburg 196140, Russia (sokolov@gao.spb.ru)

² St. Petersburg State University, St. Petersburg, Russia

Received 7 July 1999 / Accepted 22 October 1999

Abstract. The spectrophotometric variability of the magnetic CP star CU Vir in the spectral region from 1150 Å to 7850 Å is investigated. This study is based on the archival *IUE* and published visual spectrophotometric data obtained at different phases of the rotational cycle. The light variations in the wavelength region longer than λ 2000 Å are generally in antiphase to the variations in the shorter wavelength region, although the shapes of light curves are different. The existence of the “null wavelength region” at λ 2000 Å, where the amplitude of light variations is practically zero over the period of rotation, is confirmed. Moreover, the amplitudes of light variations reach the minimum values in the core of L_{α} line and in the near infrared region. The comparison of the monochromatic light curves with variations of the Si II features shows that the light variations in the far-UV are influenced by the non-uniformity of the silicon distribution over the stellar surface. The total integrated flux of CU Vir varies with phase by about 6.0%. The correlation between the total integrated flux and the magnetic field variations is discussed.

Key words: stars: atmospheres – stars: chemically peculiar – stars: fundamental parameters – stars: individual: HD 124224

1. Introduction

The light variability of Magnetic Chemically Peculiar (henceforth CP2 stars, following Preston 1974) stars can be generally explained by the variable overabundance of several heavy elements observed in the atmospheres of these stars. This mechanism arises from a non-uniform distribution of elements over the surface of the star. Enhanced energy blocking decreases the flux in the far-UV region where most of the lines of these elements are present. The blocked flux appears in the visual and the red part of the spectrum. Such an explanation is supported by the antiphase relationship of light curves in the visual and the far-UV spectral regions.

It is not obvious that this mechanism is the only one to be responsible for photometric variations, although the existing evidence strongly suggests that flux redistribution can explain the major variations seen in these stars. The influence of the

magnetic field on the atmosphere structure was quantitatively discussed by Stepień (1978). He calculated the stellar atmosphere structure taking into account the magnetic pressure term in the hydrostatic equilibrium. One of the most important results of Stepień’s calculations is that the magnetic force makes the star prolate or oblate with a difference of the polar and equatorial radii up to 3%. The distortion leads to small variations of the effective temperature over the surface. Several attempts were made to interpret the light variations of CP2 stars as a consequence of an oblate or prolate configuration: see, for example, Molnar(1974) for *a* Cen and Böhm-Vitense & Van Dyk (1987) for α^2 CVn. Moreover, the infrared variability of some CP2 stars can be interpreted by the distorted figure of these stars (Catalano & Leone 1998).

Stepień & Czechowski (1993) investigated the spectrophotometric behavior of the rapidly rotating CP2 star 56 Ari, using the archival *International Ultraviolet Explorer* (*IUE*) data and the published visual spectrophotometric data. They showed that the total integrated flux of this star varies with phase by about 2.5%. Detailed investigation of several additional stars is necessary to draw a definite conclusion about the mechanism of light variations in CP2 stars. Another rapidly rotating CP2 star wealthy in photometric and spectrophotometric data is CU Virginis (HR 5313, HD 124224). The star displays well determined periodic variations of hydrogen, helium and silicon lines. Good photometric, magnetic field and radial velocity observations are available in the literature. Molnar & Wu(1978) reported the ultraviolet photometric observations with the ANS satellite for CU Vir. The visual scans of CU Vir at different phases were obtained by White et al. (1980) and Pyper & Adelman (1985). They can be merged with the UV scans from the *IUE* archive. This allows one to investigate the spectrophotometric variations with rotational period in the spectral region from 1150 Å to 7850 Å. Moreover the total integrated flux variations for CU Vir can be also examined. This is done in the present paper.

2. Observational data

2.1. The period variations

The rotational period of CU Vir has been studied by Deutsch (1952), Hardie(1958), Peterson (1966), Blanco & Catalano (1971) and Winzer (1974). It appears that a period of

* Based on INES data from the IUE satellite.

Table 1. List of the spectral *IUE* observations of CU Vir

<i>IUE</i>	images	Julian date 2,440,000+	Phase
LWR	3443	3883.90609	0.100
LWR	3445	3883.94638	0.178
LWR	3446	3883.98738	0.256
LWR	3447	3884.03271	0.343
LWR	3448	3884.07599	0.427
LWR	3449	3884.11679	0.505
SWP	3863	3883.88328	0.056
SWP	3864	3883.91221	0.112
SWP	3865	3883.95255	0.189
SWP	3866	3883.99435	0.270
SWP	3867	3884.03750	0.353
SWP	3868	3884.08043	0.435
SWP	3869	3884.12172	0.514
LWR	4044	3949.79617	0.647
LWR	4045	3949.83722	0.726
LWR	4046	3949.87819	0.804
LWR	4047	3949.91787	0.881
LWR	4048	3949.95900	0.960
SWP	4670	3949.80036	0.655
SWP	4671	3949.84244	0.736
SWP	4672	3949.88249	0.813
SWP	4673	3949.92211	0.889
SWP	4674	3949.96452	0.970

0.520675 ± 0.000005 days is consistent with all the observations. On the other hand, Adelman et al. (1992) refined the period of CU Vir, using the *UBV* data consisting of 357 values obtained over a span of some 26 months. They found the period of 0.5206800 ± 0.0000005 days. Adelman et al. (1992) compared several independent photometric studies of CU Vir and found that the light curves taken at different epochs by various investigators show clear differences. Recently, Pyper et al. (1998) studied all possible variations for this star from 1956 to 1997. They found that all observational data might be fitted using two periods. For observational data with $JD < 2446000$ they adopted the following ephemeris:

$$JD(U, B \text{ min}) = 2435178.6417 + 0.5206778E \quad (1)$$

and for observational data with $JD > 2446000$ they found a slightly longer period using the same zero epoch:

$$JD(U, B \text{ min}) = 2435178.6417 + 0.52070308E. \quad (2)$$

Moreover, the authors noted that there was an indication of a continually changing period. The possible mechanism of an abrupt change of period of CU Vir was proposed by Stepień (1998). He noted that if one abandons the assumption of rigid rotation, the strength of the observed magnetic field is sufficient to modify the moment of inertia of the outer envelope of the star by the required amount. On the other hand, North (1998) pointed out that any explanation for this intriguing discovery would have to take into account the unevolved state of CU Vir. However, Stepień (1998) noted that the observed change of period cannot be connected with evolutionary changes of the star because

of the vast difference between the observed and expected time scale of the change.

As one can see, the situation in the determination of the period variations for CU Vir is sufficiently puzzling. Nevertheless, in our investigation the phases for the observational data with $JD < 2446000$ were computed by using Eq. (1), and for these with $JD > 2446000$ by using Eq. (2).

2.2. *IUE* scans

Eleven low-dispersion spectra of CU Vir have been recorded with *IUE* in the spectral range 200–320 nm with the large aperture (camera LWR) and twelve in the domain 115–200 nm (camera SWP) with the large aperture as well. All images of CU Vir were obtained 10 January 1979 and 17 March 1979 and are listed in Table 1 with the date of the observation. The values of phases were computed from Eq. (1). The spectra were received from the *IUE* database and the data are calibrated using standard reduction techniques described by Garhart et al. (1997). The spectra have a limiting resolution in the range 6–7 Å. Unfortunately, the data in the spectral range between 3080 Å and 3200 Å was not included in our investigation, because of the large uncertainty of the flux.

2.3. Visual scans

The visual spectrophotometric scans of CU Vir were taken from the catalog of Adelman et al. (1989). The spectrophotometry of CU Vir was carried out at Mt. Wilson Observatory in 1972 by White and at Kitt Peak National Observatory in 1972–1974, 1977 and 1981 by Pyper and Adelman. The information on the telescope-instrument combination and the journal of observations for CU Vir were given by White et al. (1980) and by Pyper & Adelman (1985). The total number of visual scans for this star is forty-nine. Unfortunately, there were systematic differences in the ultraviolet measurements obtained by various authors (Pyper & Adelman 1985). In order to exclude these systematic differences, in our study only scans obtained with the HCO Scanner on the 92-cm telescope at Kitt Peak National Observatory were used. Table 2 gives for each scan its number, the date of the observation and its corresponding phase obtained by using Eq. (1).

The observations were reduced to absolute units with a standard procedure, using the absolute calibration of *uvby* filters of Strömgren photometry obtained by Straižys & Kurilienė (1975). They established that the flux from the star (Sp: A0 V, V=0.^m0) is equal to $3.7 \times 10^{-9} \text{ erg s}^{-1} \text{ cm}^{-2} \text{ Å}^{-1}$ in the *y* filter of Strömgren system. Unfortunately, the photometric observations of CU Vir were not always reduced to the *uvby* system.

The *uvby* photometry of CU Vir was made by Weiss et al. (1976), but their data are published only as plots. The four-color and H_{β} -photometry of this star was published by Pyper & Adelman (1985). Recently, the differential four-color photometry was obtained in 1991–1997 and the data are given in the paper by Pyper et al. (1998). In order to calibrate the visual spectra, the *y* magnitudes of CU Vir based on measurements

Table 2. List of the visual spectrophotometric scans of CU Vir

Scan No.	Julian date 2440000+	Phase
11	1401.8890	0.204
12	1404.8790	0.946
13	1417.8780	0.912
17	1794.8150	0.847
18	1795.8940	0.919
19	1796.8880	0.829
20	1847.7330	0.480
21	2111.9650	0.957
22	2142.9280	0.424
23	2143.9370	0.362
24	2144.9360	0.280
25	2145.8880	0.109
26	2202.7110	0.241
27	2203.7430	0.223
28	2207.7230	0.867
29	2208.7170	0.776
30	3230.9040	0.962
31	3232.8900	0.776
32	3583.9169	0.949
33	4648.9738	0.469
34	4649.0112	0.541
35	4651.9212	0.130
36	4651.9406	0.167
37	4651.9725	0.228
38	4651.9891	0.260
39	4652.0188	0.317
40	4653.9082	0.946
41	4653.9329	0.993
42	4653.9487	0.024
43	4654.8911	0.834
44	4654.9096	0.869
45	4654.9323	0.913
46	4655.0252	0.091
47	4655.8714	0.716
48	4655.8902	0.752
49	4655.9093	0.789

from Pyper & Adelman (1985) were used, because these observations and the observations of visual spectra were obtained in close epochs. The shapes of the light curves in other filters were used to check the calibration procedure. Moreover, the visual scans calibrated with these values produced the smoothest transition to the UV scans. It should be noted that the phases for the *uvby* data were computed using the corrected JD values for CU Vir published by Adelman et al. (1992).

2.4. Spectral data

CU Vir shows relatively large variations in hydrogen, silicon and helium lines with the period of light variations. The variations of equivalent width of lines have been studied by various investigators over 40 years. Table 1 of the paper by Pyper et al. (1998) contains information on all the photometric, spectroscopic, radial velocity and magnetic field data for CU Vir

together with references to the authors. The spectral variations in lines of CU Vir have been interpreted as a result of the non-uniform distribution of elements over the surface of the rotating star. Goncharskij et al. (1983) and Hatzes (1997) produced Si-maps for CU Vir by using different spectroscopic observations. Hiesberger et al. (1995) derived a map of the helium surface distribution for this star. Borra & Landstreet (1980), using the Balmer line polarimeter for measurement of the effective magnetic field, established that CU Vir is also a magnetic variable. Recently, Pyper et al. (1998) published new observations of the effective magnetic field with the Stokesmeter and CCD detector using Si II $\lambda\lambda 6347.09$ and 6371.36 lines. The effective magnetic field measurements presented in these papers were used in our study. The value of the phases for observations obtained by Borra & Landstreet (1980) and Pyper et al. (1998) were calculated from Eqs. (1) and (2), respectively.

3. Data analysis

To analyse the *IUE* spectra of CU Vir we used a linearized least-squares method. An attempt was made to describe the light curves in a quantitative way by adjusting a Fourier series. This method is described by North (1987) and assumes that the curve has the form:

$$F(\lambda, t) = A_0(\lambda) + \sum_{i=1}^n A_i(\lambda) \cos(\omega i(t - t_0) + \phi_i(\lambda)) \quad (3)$$

where $\omega=2\pi/P$ and P is the period. The coefficients $A_0(\lambda)$ of the fitted curves give the mean flux distribution over the cycle of the variability. From several scans distributed over the period one can produce light curves at different wavelengths. Experience showed that in all cases the data could be fitted by Fourier series limited to $n=2$, i.e. by the fundamental frequency and its first harmonic. A least-squares fit was applied to all the short-wave and long-wave *IUE* monochromatic light curves. For the analysis of the visual spectra of CU Vir the same procedure was used.

3.1. The average flux distribution

The average flux distributions of short-wave and long-wave scans are plotted as the solid line in the upper and lower parts of Fig. 1, respectively. The error bars in Fig. 1 indicate the amplitude variations of the fundamental frequency. As one can see from Fig. 1, the largest changes of the flux for CU Vir are in the short-wavelength range of *IUE* spectra. The variability of the flux in the long-wavelength range of *IUE* spectra is up to 10 times smaller. On the other hand, there are no significant changes of the flux at $\lambda 2000 \text{ \AA}$. The amplitude of the light variations reaches the minimum value of 0.4%. This is in good agreement with estimates obtained by Molnar & Wu (1978). They established a possible “null wavelength region” near 2000 \AA ($\pm 100 \text{ \AA}$) where the amplitude of light variations is zero over the period of rotation. It should be noted that the flux in the core of L_α line varies with the small amplitude of 9% at $\lambda 1213 \text{ \AA}$. However the wings of this line vary significantly.

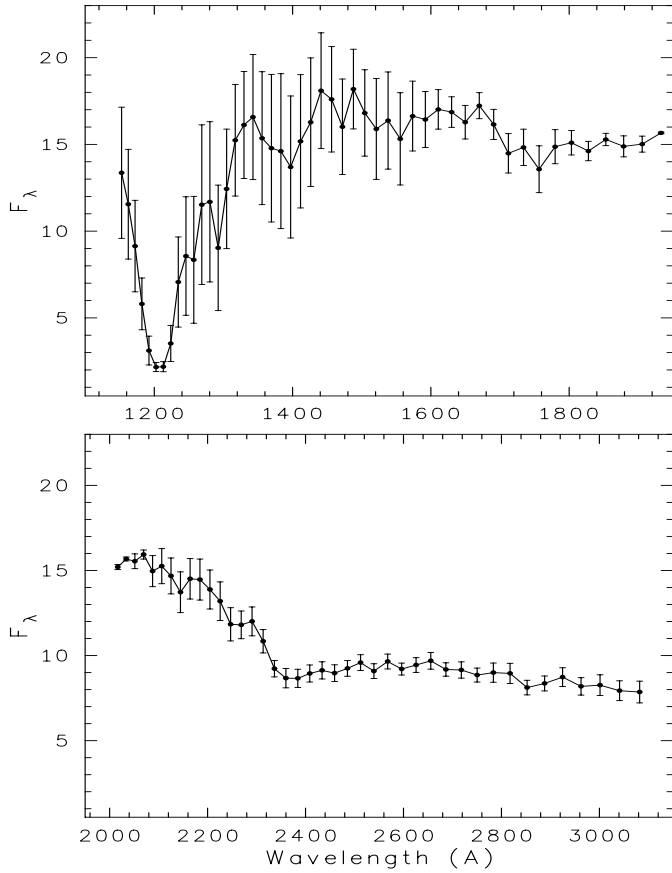


Fig. 1. The average flux distribution in $10^{-11} \text{erg s}^{-1} \text{cm}^{-2} \text{Å}^{-1}$ for CU Vir. The top and bottom panels show the short-wave and long-wave scans from the *IUE* archive, respectively.

The average visual flux distribution is plotted as the solid line of Fig. 2. In order to show the accuracy of the calibration procedure for visual scans, the long-wavelength range of the *IUE* spectra is also plotted on Fig. 2. Well-known from the *uvby* photometry, the variation of the flux in the visual part of spectrum of CU Vir decreases with the increase of the wavelength. In fact, the largest amplitude of light variations is in the Balmer continuum and the smallest amplitude is in the near infrared. The amplitude reaches the value of 6–7% around $\lambda\lambda 7530\text{--}7850 \text{ Å}$, as illustrated by Fig. 2.

3.2. The monochromatic light variations

The monochromatic light curves of CU Vir change their shape with wavelength. Examples of light curves together with the fitted two-frequency cosine curves are shown in Fig. 3. The units for the flux in Fig. 3 are the same as in Figs. 1 and 2, but in order to exclude overlapping of some curves the vertical shift on the constant value was used. In this way, the curves at $\lambda\lambda 1556, 1734, 2486, 2888 \text{ Å}$ were shifted up on the value $+1.0 \times 10^{-11} \text{erg s}^{-1} \text{cm}^{-2} \text{Å}^{-1}$. The curves at $\lambda\lambda 5000, 2000$ and 7530 Å were shifted up on the values $+2.0, +4.0$ and $+5.0 \times 10^{-11} \text{erg s}^{-1} \text{cm}^{-2} \text{Å}^{-1}$ respectively. On the other hand,

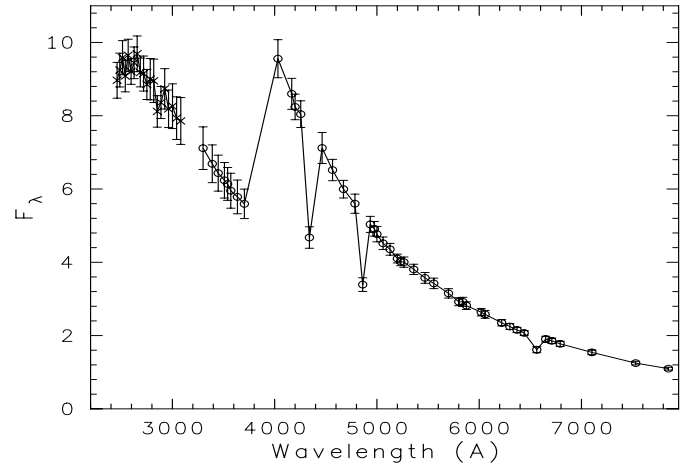


Fig. 2. The average visual flux distribution (circles) in $10^{-11} \text{erg s}^{-1} \text{cm}^{-2} \text{Å}^{-1}$ for CU Vir together with the long wavelength part of the *IUE* spectra (crosses).

the curves at $\lambda\lambda 1574, 1611, 1933, 1962, 2088$ and 2106 Å were shifted down on the values $-2.0, -5.0, -2.0, -4.0, -1.0$ and $-3.0 \times 10^{-11} \text{erg s}^{-1} \text{cm}^{-2} \text{Å}^{-1}$ respectively.

All curves in the spectral region with $\lambda \leq 1556 \text{ Å}$ have a similar shape: a deep minimum at phase 0.3–0.4 and a “hump” at phase 0.6–0.7, except for the core of L_{α} line. The light curve at $\lambda 1397 \text{ Å}$, where there is the minimum of the broad feature at $\lambda 1400 \text{ Å}$, conforms to this general trend. The amplitude of the minimum decreases with increasing wavelength. At $\lambda 1556 \text{ Å}$ the minimum and the “hump” become equally deep, but at $\lambda 1611 \text{ Å}$ and beyond, the minimum at phase 0.3–0.4 is quickly replaced by a maximum. This maximum is seen up to $\lambda 2000 \text{ Å}$. The “hump” at phase 0.6–0.7, decreases with increasing wavelength, becomes a minimum and then disappears at $\lambda 1962 \text{ Å}$. At $\lambda 1933 \text{ Å}$ the amplitude of the two features is the same and, as a result, a double wave is seen at this wavelength.

At $\lambda 2000 \text{ Å}$ there is the “null wavelength region”, where the amplitude of light variations is zero over the period of rotation. After the “null wavelength region”, the double wave suddenly appears again. The maximum of amplitude variations of this double wave is at $\lambda 2069 \text{ Å}$, but the maximum at phase 0.8 quickly disappears (see $\lambda 2106$ and beyond). As a result, the monochromatic light curves show one maximum in the spectral range of $\lambda\lambda 2106\text{--}3509 \text{ Å}$. In other words, the variations of the flux in this spectral region are in antiphase to the first minimum in the shortest wavelength region. Moreover, the maximum of light curves moves with increasing wavelength, except for the $\lambda 2486 \text{ Å}$ curve, which is essentially identical to the light curve at $\lambda 4200 \text{ Å}$ (the core of the strong Si II doublet at $\lambda 4128\text{--}30 \text{ Å}$). The maximum of light curves at $\lambda 2106 \text{ Å}$ and at $\lambda 3509 \text{ Å}$ is at phases 0.4 and 0.6, respectively. The general appearance of the light curves in the visual region is similar to that in the spectral range $\lambda\lambda 2106\text{--}3509 \text{ Å}$, although the scatter is considerable. In addition, the comparison of the obtained light curves with the differential four-color photometry published by Pypser et al. (1998) shows the similar shapes of these curves.

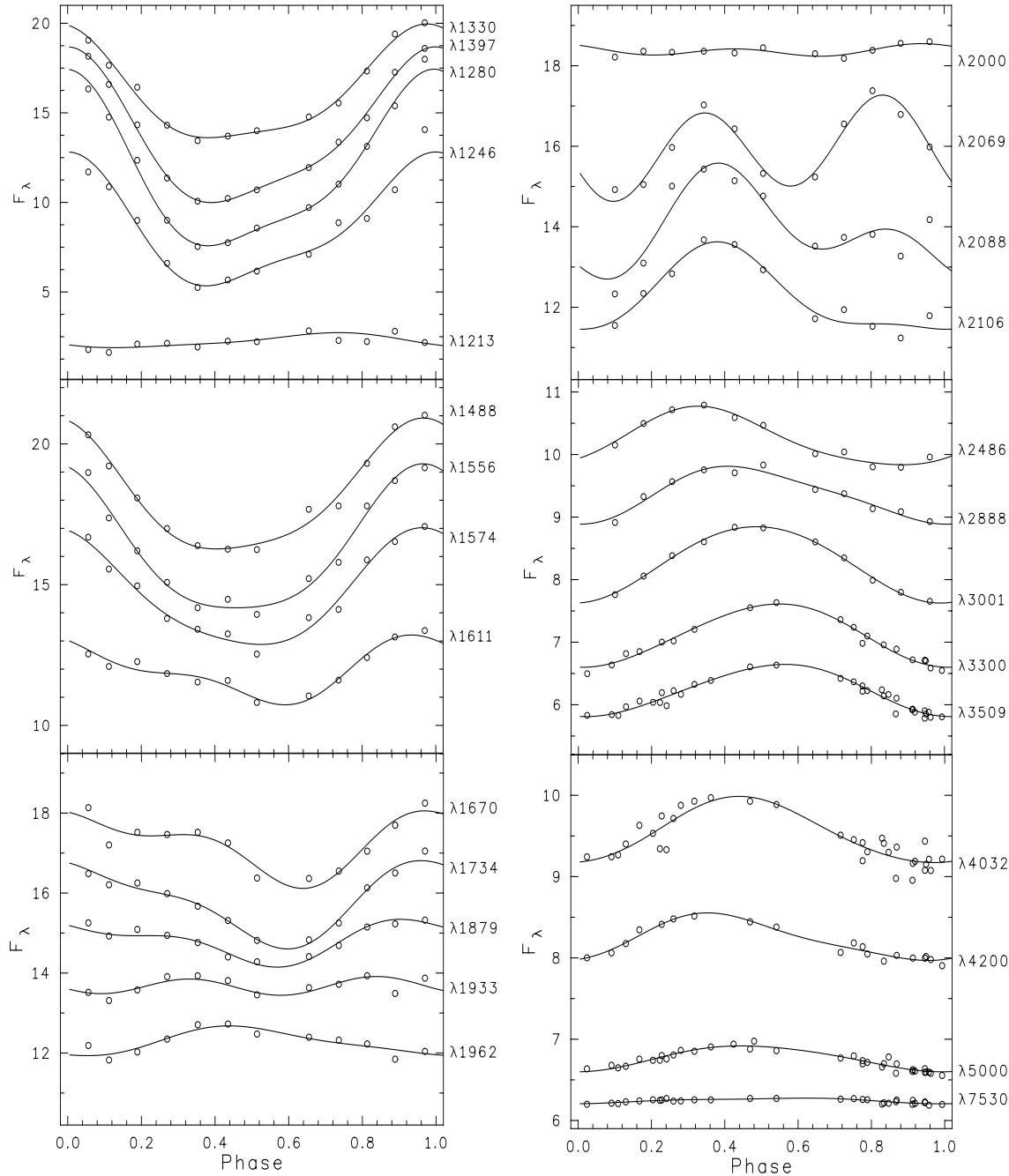


Fig. 3. Phase diagrams of the monochromatic light curves for CU Vir. To exclude the overlap the vertical shift on the constant value of some curves was used (see text). Note the different vertical scales for each part of the figure. The solid lines are the least square fits.

3.3. Variations of the UV features

The spectrum in the far UV of a silicon-rich B and early A-type stars is dominated by Si II features (Artru et al. 1981). Recently, Lanz et al. (1996) have shown that the effect of Si⁺ becomes dramatic: the Si II continuum opacity is comparable to the H I opacity at many frequencies and allows reproducing the most characteristic UV features of these stars. They established that the broad features at 130 nm, 140 nm, 156 nm and 178 nm in the spectra of CP2 stars are mainly due to Si II autoionization transitions. The characteristic flux deficiency at $\lambda 1400 \text{ \AA}$ is well

seen in the spectrum of CU Vir. Moreover, the average flux distribution is reproduced, especially between 1250 and 1850 \AA , most of the important features by taking into account the Si II continuum opacity as calculated by Lanz et al. (1996) and another more diffuse depression around $\lambda 2400 \text{ \AA}$ (see Fig. 1).

To measure the broad features at $\lambda 1400 \text{ \AA}$, Jamar et al. (1978) introduced the photometric index δ_{1400} , using TD-1 low resolution spectra. The *IUE* spectra with the high and low dispersion modes were used by Maitzen (1980, 1984) and by Shore & Brown (1987) to form the photometric indices Δa and a_{1400} ,

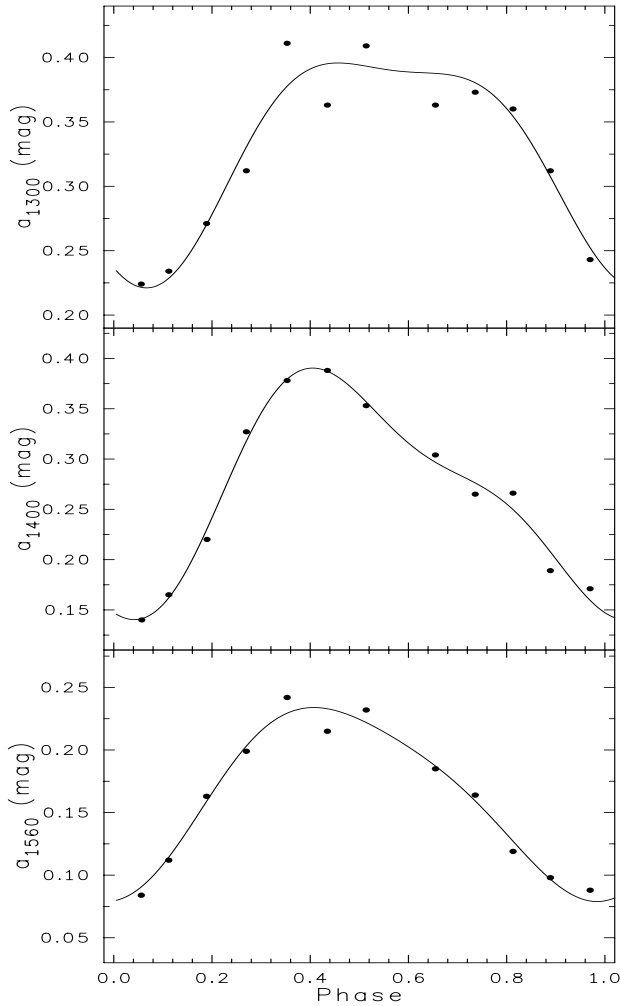


Fig. 4. The phase diagrams of the broad features in the far-UV spectral region of CU Vir. The solid lines are the least square fits.

respectively. In order to derive the total absorption in the broad features at 130 nm, 140 nm and 156 nm, we introduce the photometric indices a_{1300} , a_{1400} and a_{1560} . These indices are analogous to the a_{1400} index of Shore & Brown (1987), and are given by:

$$\begin{aligned}
 a_{1300} &= \frac{1}{2}(m_{1280} + m_{1304}) - m_{1292}, \\
 a_{1400} &= \frac{1}{2}(m_{1342} + m_{1441}) - m_{1397}, \\
 a_{1560} &= \frac{1}{2}(m_{1488} + m_{1610}) - m_{1555}.
 \end{aligned}
 \tag{4}$$

The depressions at 178 nm and 240 nm were excluded, since these depressions are very wide in the spectra of CU Vir.

Fig. 4 exhibits the variations of the measured total absorption for the three broad features versus the rotational phase. The solid lines represent least-squares fits by two-frequency cosine functions. It can be seen on the graphs of Fig. 4 that all photometric indices have minimum values at phase 0.0 and maximum values at phases 0.4 and 0.7, although the shapes of the fitted curves, especially after the first maximum, are different. The

comparison of the light variations in the far-UV and the variations of silicon features shows that they vary in antiphase. This agrees with the anticorrelation supported by the energy blocking mechanism in the far-UV for CP2 stars.

4. The total integrated flux

The method proposed by Stepień & Dominiczak (1989) to use *IUE* measurements from $\lambda 1150 \text{ \AA}$ to $\lambda 3200 \text{ \AA}$ and the visual spectrophotometry from $\lambda 3300 \text{ \AA}$ to $\lambda 7850 \text{ \AA}$, is taken to compute the total integrated flux of CU Vir. The missing fluxes, i.e. the fluxes radiated outside of the observed interval, can be estimated and added to the respective observed fluxes. The fluxes for $\lambda \leq 1150 \text{ \AA}$ and for $\lambda \geq 7850 \text{ \AA}$ were found from Kurucz model with $T_{\text{eff}}=13000 \text{ K}$ and $\log g=4.0$ and the flux for $3200 \leq \lambda \leq 3300 \text{ \AA}$ was found from a linear interpolation between the *IUE* and visual data. The fraction of the total energy flux in the interval 1150–7850 \AA is close to 90%. The total integrated flux computed from the mean energy distribution of CU Vir is equal to $4.62 \times 10^{-7} \text{ erg s}^{-1} \text{ cm}^{-2}$. This value is slightly less than the value computed by Lanz (1984) which is equal to $5.45 \times 10^{-7} \text{ erg s}^{-1} \text{ cm}^{-2}$.

To compute the total integrated flux at each phase, the coefficients of the fitted curves in the observed spectral regions were used. Moreover, the coefficients of the missing fluxes for extreme UV ($\lambda \leq 1150 \text{ \AA}$) were extrapolated by a straight line, assuming zero flux at wavelengths shorter than the Lyman discontinuity. The coefficients of the fitted curves for $3200 \leq \lambda \leq 3300 \text{ \AA}$ were found from a linear interpolation of the coefficients between the *IUE* and visual data. On the other hand, it was assumed that the added missing fluxes for $\lambda \geq 7850 \text{ \AA}$ do not vary with phase. This procedure allows to minimize the uncertainty of the individual measurements and to compute the total integrated flux at each phase. The top panel of Fig. 5 shows the variation of the relative bolometric magnitude (BC) over the period of rotation. As one can see from Fig. 5, BC has two maxima at phases 0.4 and 0.95 and two minima at phases 0.1 and 0.7. The difference of the bolometric magnitudes at phases 0.4 and 0.7 is equal to 6%. The deep minimum of the flux at phase 0.6–0.7 (see. Fig. 3) for $\lambda \leq 2000 \text{ \AA}$ is not compensated for by the maximum for $\lambda > 2000 \text{ \AA}$ and, as a result, the minimum of BC is seen at this phase.

To explain the total integrated flux variations there are two possibilities. First of all, the magnetically distorted photosphere predicted by Stepień (1978) may exist in CU Vir. In this way, the correlation between the total integrated flux variations and the effective magnetic field variations can be understood. The bottom panel of Fig. 5 shows the variation of the effective magnetic field over the period of rotation. The comparison of the BC variations with the effective magnetic field variations supports the atmosphere structure for the magnetic stars proposed by Stepień (1978), because the maximum of the BC corresponds to the phase where the magnetic field lines are mainly horizontal and two minima of the BC corresponds to the phases where the field lines basically are vertical to the stellar surface. It should be noted that there is a difference in the bolometric magnitudes

at phases 0.1 and 0.7 (two minima) which is equal to 2.5%. This difference is consistent with a magnetic dipole of CU Vir whose axis is decentered by about 0.2 of the stellar radius along the dipole axis (Hatzes 1997).

Second, effective temperature variations over the rotational cycle may exist in CU Vir. Several attempts were made in the past to explain the observed amplitudes of photometric and spectroscopic variations by variations of the effective temperature for CU Vir. Weiss et al. (1976) suggested effective temperature variations with the amplitude of 600 K, as well as surface gravity variations. Ryabchikova (1991) noted that all spectroscopic variations including those of the hydrogen line cores can be explained in the frame of the oblique rotator model with inhomogeneous abundance and temperature distribution over the stellar surface. The resulting temperature and gravity differences are in good agreement with those of Weiss et al. (1976), but the position of the hot region is shifted in phase compared with theirs. In both cases the hot regions do not correspond to the maximum of the BC. The new method for the effective temperature determination proposed by Sokolov (1998) can be a useful tool to study the inhomogeneous temperature distribution over the surface of CU Vir.

5. Conclusions

The archival *IUE* and published visual spectrophotometric observations of CU Vir have permitted to analyse the light variations of CU Vir at various wavelengths. The light variations in the wavelength region longer than $\lambda 2000 \text{ \AA}$ are generally in antiphase to the light variations in the shorter wavelength region. However the minimum at phase 0.6–0.7 of the monochromatic light curves with $\lambda < 2000 \text{ \AA}$ is not compensated for by the maximum in the longer wavelength region. The brightness of the star at $\lambda 2000 \text{ \AA}$ is constant over the period of variations which means that the so called “null wavelength region” exists for CU Vir. Moreover, the amplitudes of light variations reach the minimum values in the core of L_α line and in the near infrared region, where the flux is formed in the outer layers of the stellar atmosphere.

The variable broad features in the far-UV connected with a non-uniform distribution of silicon over the surface of CU Vir influence substantially the light variations in the UV. The anti-correlation between the light variations in the far-UV and the silicon features variations is caused by extra blocking of the flux in the far-UV and its redistribution in the longer wavelengths. But this is not the only mechanism for the light variations of CU Vir. The present data suggest variations of the total integrated flux of CU Vir with the amplitude of 6%. The correlation between the total integrated flux variations and the effective magnetic field variations can be interpreted as a result of the distorted shape of this star. However this result needs an independent confirmation.

Acknowledgements. The author would like to thank Dr. T. Ryabchikova for providing the observational data of CU Vir in electronic form. This work has been supported by the Russian National Foundation for Astronomy (project No. 1. 4. 1. 2).

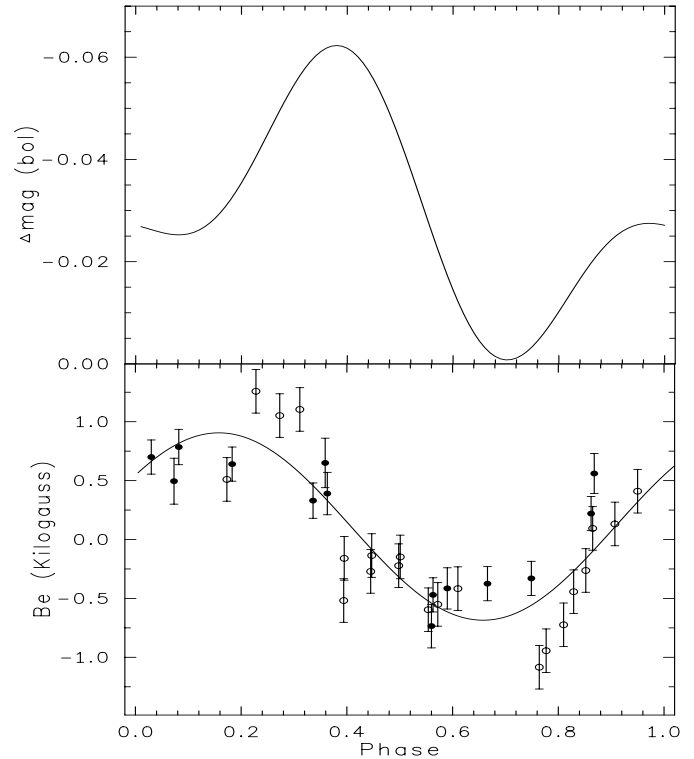


Fig. 5. The total integrated flux and the effective magnetic field variations of CU Vir. The top panel shows the relative bolometric magnitude variations. The bottom panel displays the effective magnetic field variations observed by Borra & Landstreet (1980) (filled circles) and by Pyper et al. (1998) (open circles). The solid line on the bottom panel is the least square fit by cosine wave.

Note: Kuschnig et al. (1999) reported on the $\log g$ variations for CU Vir from fitting the H_δ line profiles at phases of maximum and minimum line strength with models of the same effective temperature.

References

- Adelman S.J., Pyper D.M., Shore S.N., White R.E., Warren W.H., 1989, *A&AS* 81, 221
- Adelman S.J., Dukes R.J., Pyper D.M., 1992, *AJ* 104, 314
- Artru M.C., Jamar C., Petrini D., Praderie F., 1981, *A&A* 96, 380
- Blanco C., Catalano F., 1971, *AJ* 76, 630
- Böhm-Vitense E., Van Dyk S.D., 1987, *AJ* 93, 1527
- Borra E.F., Landstreet J.D., 1980, *ApJS* 42, 421
- Catalano F.A., Leone F., 1998, In: North P., Žižňovský J. (eds.) European Working Group for CP stars. 26th Workshop, *Contrib. Astron. Obs. Skalnaté Pleso* 27, p. 243
- Deutsch A.J., 1952, *ApJ* 116, 536
- Garhart M.P., Smith M.A., Levay K.L., Thompson R.W., 1997, *NASA IUE Newsl.*, 57
- Goncharskij A.V., Ryabchikova T.A., Stepanov V.V., Khokhlova V.L., Yagola A.G., 1983, *SvA* 27, 49 (in Russian)
- Hardie R., 1958, *ApJ* 127, 620
- Hatzes A.P., 1997, *MNRAS* 288, 153
- Hiesberger F., Piskunov N., Bonsack W.K., et al., 1995, *A&A* 296, 473
- Jamar C., Macau-Hercot D., Praderie F., 1978, *A&A* 63, 155

- Kuschnig R., Ryabchikova T.A., Piskunov N.E., Weiss W.W., Gelbmann M.J., 1999, A&A 348, 924
- Lanz T., 1984, A&A 139, 161
- Lanz T., Artru M.C., Dourneuf M.Le., Hubeny I., 1996, A&A 309, 218
- Maitzen H.M., 1980, A&A 84, L9
- Maitzen H.M., 1984, A&A 138, 493
- Molnar M.R., 1974, ApJ 187, 531
- Molnar M.R., Wu C.C., 1978, A&A 63, 335
- North P., 1987, A&AS 69, 371
- North P., 1998, A&A 334, 181
- Peterson B.A., 1966, ApJ 145, 735
- Preston G.W., 1974, ARA&A 12, 357
- Pyper D.M., Adelman S.J., 1985, A&AS 59, 369
- Pyper D.M., et al., 1998, A&A 339, 822
- Ryabchikova T.A., 1991, In: Tuominen I., et al. (eds.) The Sun and Cool stars: Activity, Magnetism, Dinamos. IAU Coll. 130, Lecture Notes in Physics 380, Springer, p. 350
- Shore S.N., Brown D.N., 1987, A&A 184, 219
- Sokolov N.A., 1998, A&AS 130, 215
- Stepień K., 1978, A&A 70, 509
- Stepień K., 1998, A&A 337, 754
- Stepień K., Czechowski W., 1993, A&A 268, 187
- Stepień K., Dominiczak R., 1989, A&A 219, 197
- Straižys V., Kurilienė G., 1975, Bull. Vilnius Obs. 42, 16
- Weiss W.W., Albrecht R., Wieder R., 1976, A&A 47, 423
- White R.E., Pyper D.M., Adelman S.J., 1980, AJ 85, 836
- Winzer J.E., 1974, Ph.D. Thesis, Univ. Toronto